Title

Inhibition of Mul1-mediated ubiquitination promotes mitochondria-associated translation

Authors

Yuan Gao[1], Maria Dafne Cardamone[1], Julian Kwan[1,2], Joseph Orofino[1], Ryan Hekman[1,2], Shawn Lyons[1], Andrew Emili[1,2,3], Valentina Perissi[1,4]

[1] Biochemistry Department, Boston University School of Medicine, Boston, MA 02115

[2] Center for Network and Systems Biology, Boston University, Boston, MA 02115

[3] Biology Department, Boston University, Boston, MA 02115

[4] Corresponding Author

Keywords

Ubiquitin, GPS2, mitochondria, PABPC, Mul1, mitochondria stress response (MSR)

Running title

Regulation of mitochondria-associated translation by GPS2

ABSTRACT

G-Protein Pathway Suppressor 2 (GPS2) was recently identified as an endogenous inhibitor of non-proteolytic ubiquitination mediated by the E2 ubiquitin-conjugating enzyme Ubc13. GPS2-mediated restriction of K63 ubiquitination is associated with the regulation of insulin signaling, inflammation and mitochondria-nuclear communication, however a detailed understanding of the targets of GPS2/Ubc13 activity is currently lacking, Here, we have dissected the GPS2-regulated K63 ubiquitome in mouse embryonic fibroblasts and human breast cancer cells, unexpectedly finding an enrichment for proteins involved in RNA binding and translation. Characterization of putative targets, including the RNA-binding protein PABPC1 and translation factor eiF3m, revealed a strategy for regulating the mitochondria-associated translation of selected mRNAs via Mul1-mediated ubiquitination. Our data indicate that removal of GPS2-mediated inhibition, either via genetic deletion or stress-induced nuclear translocation, promotes the ubiquitination of mitochondria-associated translation factors leading to increased expression of an adaptive antioxidant program. In light of GPS2 role in nuclear-mitochondria communication, these findings reveal an exquisite regulatory network for modulating mitochondrial gene expression through spatially coordinated transcription and translation.

INTRODUCTION

Maintenance of mitochondria metabolism and energy homeostasis is guaranteed by a constant turnover of the mitochondrial network, including both generation of new mitochondria, remodeling of existing mitochondria and removal of damaged organelles[1]. Mitochondria biogenesis and rewiring of mitochondrial functions require coordinated gene expression from the mitochondrial and nuclear genomes[2–5]. This is achieved through energy-sensing signaling pathways impacting on the transcriptional network controlling the expression of nuclear-encoded mitochondrial genes, and via shuttling of transcription factors and cofactors between the two organelles[6–9]. In yeast, balanced expression of different OXPHOS subunits is also facilitated by synchronized control of mitochondrial and cytosolic translation[2,10–13], suggesting that coordinated regulation of multiple levels of gene expression may be required for the maintenance of mitochondrial homeostasis. However, the molecular mechanisms promoting balanced mitochondrial gene expression and specific mRNA processing and translation at the level of single organelles in mammals are not yet fully understood. Recent studies have identified RNA-binding proteins responsible for recruiting selected mRNAs to the mitochondrial outer membrane surface[14–23], providing some clues to the specificity of translation on mitochondria-associated ribosomes as compared to cytosolic ribosomes. However a complete understanding of the modes of regulation of mitochondria-associated translation is currently lacking.

Ubiquitination is a reversible protein post-translational modification that is achieved through the sequential actions of several classes of enzymes, including a ubiquitin (Ub)-activating enzyme (E1), a Ub-conjugating enzyme (E2), and a Ub ligase (E3), that work together to mediate the attachment of one or multiple ubiquitin moieties to lysine residues on target proteins[24,25]. In the case of poly-ubiquitination, chains of different topology can either promote protein degradation or serve, as in the case of other post-translational modifications, to influence protein functions and interactions[26,27]. Among others, K48-linked ubiquitin chains are best known as markers for

69 proteasomal degradation, whereas K63-linked ubiquitin chains are non-proteolytic[28,29] and are
70 associated with immune signaling, DNA damage repair, protein sorting, and translation[30–37].
71 Moreover, more recent studies point to a broader role in regulating cellular metabolism and
72 adaptive responses to stress[38–43]. Notably, K63-linked ubiquitin mediates translational regulation
73 in yeast exposed to oxidative stress[39,42].

74 We recently identified GPS2 as an inhibitor of K63 ubiquitination synthesized by the E2
75 conjugating enzyme Ubc13[44]. GPS2-mediated inhibition of K63 ubiquitination is essential for
76 promoting several coordinated functions across the cell, including the transcriptional regulation of
77 mitochondrial genes in the nucleus and activating insulin signaling and pro-inflammatory
78 pathways in the cytosol[9,44–47]. These complementary activities across different subcellular
79 compartments are facilitated by GPS2 translocation between organelles, making GPS2 an
80 excellent candidate for mediating the coordination of nuclear and extranuclear processes
81 contributing to the remodeling of cellular metabolism. Regulated mitochondria-to-nucleus
82 shuttling of GPS2, for example, controls mitochondria biogenesis via transcriptional activation of
83 nuclear-encoded mitochondrial genes[9]. Acting as a mediator of mitochondria retrograde
84 signaling, GPS2 is also required for licensing the expression of stress response genes upon
85 mitochondria depolarization[9]. Upon translocation to the nucleus, GPS2-mediated inhibition of K63
86 ubiquitination impacts the remodeling of the chromatin environment of target gene promoters by
87 stabilizing histone demethylases[9]. At the same time, its removal from the outer mitochondrial
88 membrane may release the ubiquitination of other targets, which are currently unknown. Here,
89 we have profiled the GPS2-regulated ubiquitome and dissected the role of GPS2-regulated K63
90 ubiquitination in modulating mitochondria-associated protein translation. Our results point to a
91 novel regulatory strategy whereby GPS2 provides a unifying strategy for coordinating the
92 transcriptional and translational control of mitochondrial gene expression by inhibiting K63
93 ubiquitination of key targets by the mitochondrial ubiquitin ligase Mul1.

RESULTS

Remodeling of the mitochondrial proteome in the absence of GPS2

Our previous work has identified GPS2 as a regulator of mitochondrial gene expression, through transcriptional control of nuclear-encoded mitochondrial (neMITO) genes, and as a mediator of mitochondria-to-nucleus retrograde signaling[9]. To further dissect the role of GPS2 in regulating mitochondrial functions, we profiled the mitochondrial proteome and transcriptome of immortalized mouse embryonic stem cells (MEFs) derived from either GPS2$^{fl/fl}$/Ubc^{ERT2}-Cre^{+} or GPS2$^{fl/fl}$/Ubc^{ERT2}-Cre^{-} mice. Upon Tamoxifen treatment, GPS2 deletion is induced in Ubc^{ERT2}-Cre^{+} cells (from here on called GPS2-KO), whereas Ubc^{ERT2}-Cre^{-} (from here on called WT) serve as negative control (**Supplemental Figure S1A)**. In agreement with previous studies in other cell models, GPS2-KO MEFs present with severely reduced mitochondrial content compared to WT cells (**Supplement Figure S1B**).

To achieve a comprehensive characterization of the changes associated with GPS2 deletion, we first profiled mitochondrial extracts from WT and KO MEFs using quantitative tandem mass tag (TMT) labeling followed by quantification via mass spectrometry (LC-MS/MS). We identified 891 differentially expressed proteins across three replicates (**Supplementary Table 1**, P-value <0.05 and LogFC>0.25**)**. In accord with our previous findings in adipocytes and breast cancer cells[44,46,47], upregulated proteins were enriched for pathways previously found to be regulated by cytosolic GPS2, including EGFR/Insulin signaling, inflammatory responses, and TNFalpha/MAPK signaling (**Supplemental Table 1** and **Figure S1C**). Downregulated proteins, instead, spanned various mitochondrial functions, including Electron Transport Chain (ETC), fatty acid oxidation, TCA cycle, and amino acid metabolism (**Supplemental Table 1** and **Figure S1C**). Accordingly, filtered analysis of intrinsic mitochondrial proteins, based on the latest MitoCarta 3.0 database, indicated that the majority of differentially expressed mitochondrial proteins are

119 downregulated in GPS2-KO cells, as expected based on previous studies (**Figure 1A**)[9]. However,
120 we also identified a small subset of mitochondrial proteins upregulated in the absence of GPS2.
121 Interestingly, the upregulated program was enriched in proteins involved in antioxidant response
122 and programmed cell death (**Figure 1A**), which suggests adaptive changes in response to the
123 stress of GPS2 deletion. Upregulation of anti-oxidative protective proteins SOD2 and PRDX2,
124 fatty acid synthase FASN, and downregulation of pyruvate dehydrogenase PDHA and OXPHOS
125 proteins was confirmed by western blotting of mitochondrial extracts from GPS2 WT and KO
126 MEFs (**Figure 1B**).
127
128 To characterize the molecular mechanisms underlying the adaptive regulation of
129 mitochondrial gene expression in the absence of GPS2, we profiled mitochondria-associated RNA
130 from WT and GPS2-KO MEFs by RNA-seq. Among the differentially expressed genes (DEGs)
131 (**Supplementary Table 2**), we identified 316 mitochondrial genes consistently regulated across
132 three independent replicates, including 138 upregulated and 178 downregulated genes. Overlay
133 of the RNA-seq results over the proteomics data confirmed that the downregulation of
134 mitochondrial proteins observed in GPS2-KO cells is largely associated with reduced mRNA
135 levels (**Figure 1C**), as expected based on GPS2 acting as a required transcriptional cofactor for
136 the activation of neMITO genes[9]. Indeed, overlay of the MEFs proteomics data over GRO-seq
137 data previously generated in 3T3-L1 cells with acute GPS2 downregulation further indicates that
138 protein downregulation likely results from defective transcription (**Figure 1D**)[9]. Mitochondrial
139 proteins upregulated in GPS2-KO cells instead included genes presenting both increased (59%,
140 depicted in red in **Figure 1C**) or decreased (35%, depicted in blue in **Figure 1C**) mRNA
141 abundance in KO versus WT cells. However, a comparison of protein and nascent RNA
142 expression suggests that the transcription of the majority of proteins differentially regulated in
143 MEFs, including both up- and down-regulated genes, is impaired in the absence of GPS2 (**Figure**
144 **1D**). This suggests that multiple levels of regulation may be contributing to the remodeling of the

145 mitochondrial proteome of GPS2-KO cells, including both transcriptional repression and post-
146 transcriptional regulation of mRNA stability and/or protein synthesis, with the outcome for different
147 gene/protein sets depending on the overlay of these complementary regulatory strategies.

148 *GPS2 restricts K63 ubiquitination of mitochondrial proteins*

149 To further our understanding of the adaptive rewiring of the mitochondrial proteome in
150 GPS2-null cells, we decided to investigate the mechanism/s responsible for post-transcriptional
151 regulation of mitochondrial gene expression in the absence of GPS2. Because our previous work
152 indicates that GPS2 exerts its functions across different subcellular compartments via inhibition
153 of the ubiquitin-conjugating enzyme Ubc13[9,44–48], we focused on K63 ubiquitination as a possible
154 regulatory mechanism. First, we asked whether loss of GPS2 leads to unrestricted K63
155 ubiquitination activity on mitochondria. Indeed, we observed increased accumulation of K63
156 ubiquitin chains in mitochondrial extract from GPS2 KO cells compared to the WT line by western
157 blot analysis (**Figure 2A**). To identify putative targets of GPS2-mediated regulation, we then
158 profiled the K63 ubiquitome of GPS2 WT and KO MEFs by LC-MS/MS. Relative quantification
159 was performed by stable isotope labeling of amino acid in cell culture (SILAC) (**Figure 2B**), with
160 K63 ubiquitinated proteins being enriched prior to mass spectrometry through selective binding
161 to the high-affinity lysine-63-poly-ubiquitin binding domain Vx3K0[49] (**Supplemental Figure 2A**
162 and **2B**). This approach led to the identification of 73 candidate targets, among 230 differentially
163 enriched proteins, for which the increase in the H/L ratio indicated increased ubiquitination and/or
164 increased interaction with ubiquitinated targets in GPS2-KO cells (**Supplemental Figure 2C** and
165 **Supplemental Table 3**). Unexpectedly, we found that putative targets of GPS2-mediated
166 regulation were strongly enriched for factors involved in protein translation (**Figure 2C**), whereas
167 no significant overlap with known targets of K63 ubiquitination by Parkin was observed, despite
168 mitophagy markers being activated in GPS2-KO cells (Supplemental Figure 2D, 2E and
169 **Supplemental Table 3**). These findings were confirmed when profiling was repeated using TMT

170 labeling instead of SILAC (**Supplemental Figure 2D**). A similar enrichment in proteins involved
171 in translation and RNA processing was also observed by profiling the K63 ubiquitome of MDA-
172 MB231 breast cancer cells deleted of GPS2 (REF) (**Supplemental Figure 2E** and **Supplemental**
173 **Table 3**). Moreover, the increased ubiquitination of representative translation factors RPS11 and
174 RACK1 - both previously reported as direct targets of non-proteolytic ubiquitination (REFs) - was
175 confirmed by IP/WB using both whole-cell extracts and fractionated mitochondrial extracts
176 (**Figure 2D**). This indicates that lack of GPS2 promotes exacerbated ubiquitination of translation
177 factors associated with mitochondria, thus suggesting that GPS2-mediated inhibition of K63
178 ubiquitination might regulate mitochondria-associated protein translation.
179
180 To investigate whether protein translation is regulated in absence of GPS2, we compared
181 the rate of protein translation in WT and KO cells by monitoring the incorporation of puromycin
182 into newly synthesized proteins across subcellular compartments. A significant increase in
183 puromycin incorporation was observed in mitochondria from GPS2-KO cells compared to WT
184 (**Figure 2E**). Pre-treatment of cells with the translation initiation inhibitor homoharringtonine
185 (HHT)[50] reduced puromycin incorporation in both WT and KO mitochondria, indicative of active
186 translation. Remarkably, the increase in puromycin incorporation was specific to the mitochondrial
187 compartment, with no significant changes observed in nuclear and cytosolic extracts (**Figure 2E**).
188 Together, these results indicate that the rate of protein translation in mitochondrial extracts is
189 specifically upregulated in absence of GPS2. Based on previous studies indicating that this
190 approach allows for selective measurement of translation of nuclear-encoded mitochondrial
191 proteins occurring on the outer mitochondrial membrane (OMM) as compared to the translation
192 of mitochondria-encoded genes[51], we concluded that mitochondria-associated translation of
193 neMITO genes increases in absence of GPS2. This suggests a localized regulatory strategy
194 impacting mRNAs translated by ribosomes docked on the mitochondria rather than free cytosolic
195 ribosomes. In accord with this hypothesis, we observed that transcripts encoding for more than

196 half of the upregulated proteins in GPS2-KO cells are recruited to the outer mitochondrial
197 membrane for import-coupled translation via interaction with the AKAP1/MDI/LARP
198 complex[18,52](**Supplementary Table 1**). Conversely, no significant overlap was observed between
199 upregulated proteins in the absence of GPS2 and transcripts binding to CluH, an RNA binding
200 protein responsible for the assembly of cytosolic granules promoting the translation of a variety
201 of mitochondrial proteins[14,15,53], including several showing reduced transcription in the absence of
202 GPS2 (**Supplementary Table 1**). Together, these comparative *in silico* analyses suggest that
203 enhanced translation of mitochondrial proteins in the absence of GPS2 is specific for
204 mitochondrial transcripts translated by mitochondria-associated ribosomes.
205
206 *PABPC1 ubiquitination by Mul1*
207 To gain further mechanistic insights into the regulation of mitochondria protein translation via K63
208 ubiquitination, we focused on the poly-A binding protein PABPC1. PABPC1 is not only a known
209 target of ubiquitination[54] but also the single putative target of GPS2 regulation identified across
210 different multiple experimental setups (SILAC and TMT labeling) and different cell types (MEFs
211 and MDA-MB-231) (**Supplemental Figure 3A**). Two complementary IP/WB approaches
212 confirmed increased K63 ubiquitination of PABPC1 in the mitochondria of GPS2-KO cells. In the
213 first assay, we immunoprecipitated K63Ub-containing proteins by binding to the Vx3KO trap and
214 visualized PABPC1 by WB (**Figure 3A**). In the second, we immunoprecipitated PABPC1 and
215 visualized associated K63Ub chains by WB (**Figure 3B**). As expected, the increase in high
216 molecular weight (HMW) Ub chains observed in GPS2-KO cells was reversed by inhibiting the
217 activity of ubiquitin-conjugating enzyme Ubc13 with the chemical inhibitor NSC697923
218 (REF)(**Figure 3B**). A Ubc13-dependent increase in PABPC1 ubiquitination was also observed
219 upon depolarization of mitochondria by FCCP, a condition mimicking GPS2 downregulation
220 through its relocalization from mitochondria to the nucleus[9](**Figure 3C**). Unexpectedly, this
221 experiment revealed that FCCP-induced ubiquitination of PABPC1 depended on the mitochondria

222 specific E3 ligase MUL1 rather than MKRN1, which had been previously associated with PABPC1
223 ubiquitination in the cytosol (**Figure 3C**). Ubiquitination of PABPC1 by MUL1 and Ubc13, as
224 recapitulated *in vitro* using bacterially expressed recombinant proteins, was significantly reduced
225 upon mutagenesis of the previously identified ubiquitination sites (K78, K188, K284, and K512)
226 (**Figure 3D**) and significantly inhibited by GPS2 (**Figure 3E**). Together these results indicate that
227 PABPC1 can be locally regulated through different ubiquitination machineries and that GPS2 is
228 specifically responsible for preventing its ubiquitination by Mul1 on mitochondria.
229 PABPC1 is an RNA-binding protein and a key component of the translation machinery. PABPC1
230 concomitant interactions with the polyA-containing 3'UTR and 5' Cap-bound components of the
231 translation initiation complex promote protein translation through closed-loop mRNP
232 formation[55,56]. To unravel whether loss of GPS2 may be impacting on mitochondria-associated
233 translation through aberrant PABPC1 ubiquitination, we first asked whether PABPC1 interaction
234 with the translation initiation complex is altered in the absence of GPS2. Co-immunoprecipitation
235 experiments indicated that PABPC1 interaction with the translation initiation factor eIF4G and
236 translational activator PABP-interacting protein 1 (PAIP1) is more robust in mitochondria from
237 GPS2-KO cell than their WT counterparts (**Figure 3F)**. In contrast, interaction with the
238 translational repressor PABP-interacting protein 2 (PAIP2), which competes with PAIP1 for
239 interaction with PABP[57], is significantly decreased (**Figure 3F)**. These changes are rescued by
240 transient downregulation of the E3 ubiquitin ligase MUL1 (**Figure 3G**), indicating that aberrant
241 ubiquitination of MUL1 target/s in the absence of GPS2-mediated inhibition of Ubc13 activity is
242 indeed a contributing factor to the observed phenotype. This conclusion was further confirmed by
243 rescue of enhanced protein translation rate in GPS2-KO MEF cells through MUL1 downregulation
244 by siRNA, as measured by mitochondrial puromycilation assay (**Figure 3H**).
245 While we have primarily focused on PABPC1 due to its striking identification across multiple
246 datasets, we also considered the possibility that ubiquitination of additional factors may be
247 contributing to regulate mitochondria-associated translation. GPS2-regulated K63 ubiquitome

248 included a number or putative targets involved in RNA processing and translation. Among them,
249 eukaryotic translation initiation factor 3, subunit M (eiF3m), was also confirmed as a direct target
250 of GPS2/Ubc13/Mul1-mediated regulation (**Supplemental Figure 3B**). Our results together
251 indicate that GPS2 regulates mitochondria-associated translation by preventing aberrant MUL1-
252 mediated ubiquitination of translation factors like PABPC1 and eIF3m on the outer mitochondrial
253 membrane.
254
255 *K63ub-mediated regulation of mitochondria-associated translation in stress response*
256 Our previous studies indicate that, in conditions of mitochondrial depolarization, GPS2
257 translocates to the nucleus for regulating the transcription of stress response genes[9]. This
258 suggested that removal of GPS2 by translocation could have the indirect effect of releasing Mul1
259 activity and promoting mitochondrial protein translation as part of the adaptive stress response.
260 To investigate this possibility, we first assessed the ubiquitination of PABPC1 after depolarization
261 with FCCP for 10' or 30'. As expected, concomitant to the translocation of GPS2 from
262 mitochondria to the nucleus (**Figure 4A**), we observed a significant increase in mitochondria-
263 associated K63 poly-ubiquitination of PABPC1 (**Figure 4B** and **4C**). Under these conditions,
264 PABPC1 interaction with the translation initiation complex is strengthened (**Figure 4D**). This
265 correlates with the activation of a gene expression program that, in part, mirrors that identified in
266 response to GPS2 deletion (**Figure 4E, bottom cluster**), as validated by western blotting for
267 antioxidant proteins SOD2 (**Figure 4F**). At the same time, activation of a large part of the FCCP-
268 induced program is impaired in GPS2-KO cells, likely due to reduced transcription in the absence
269 of nuclear GPS2.
270

271 **DISCUSSION**

272

273 Previous studies have characterized GPS2 as a mediator of mitochondria retrograde signaling, a
274 transcriptional cofactor involved in mediating both gene repression and activation, and an inhibitor
275 of non-proteolytic K63 ubiquitination. Together, these complementary functions ensure a proper
276 adaptive response to mitochondrial stress and regulate mitochondria biogenesis during
277 differentiation, with GSP2 translocating from mitochondria to nucleus to regulate nuclear-encoded
278 mitochondrial genes transcription via stabilization of chromatin remodeling enzymes[9]. A key
279 implication of these findings is that restricted K63 ubiquitination in the nucleus indirectly regulates
280 mitochondrial functions through the expression of stress response and nuclear-encoded
281 mitochondrial genes. However, it remains unclear whether GPS2 also contributes to the
282 regulation of mitochondria homeostasis in a direct manner, possibly by modulating the
283 ubiquitination of mitochondrial proteins. To address this question, we have profiled the GPS2-
284 regulated K63 ubiquitome in mouse embryonic fibroblasts and human breast cancer cells. To our
285 surprise, we did not observe any significant overlap between the GPS2-regulated program and
286 the mitochondrial proteins targeted by Parkin-mediated ubiquitination. This suggests that stress-
287 induced translocation of GPS2 is unlikely to contribute to removing defective mitochondria via
288 mitophagy. Instead, GPS2-mediated inhibition of K63 ubiquitination prevalently affects proteins
289 involved in RNA processing and translation. In particular, our results indicate that GPS2-mediated
290 inhibition of K63 ubiquitination contributes to regulating the mitochondria-associated translation
291 of a specific of nuclear-encoded mitochondrial genes. Together with the previous characterization
292 of nuclear GPS2 as an essential cofactor for the expression of nuclear-encoded mitochondrial
293 genes, these findings indicate that GPS2-mediated inhibition of K63 ubiquitination represents a
294 unifying strategy for modulating the expression of mitochondrial proteins through coordinated
295 transcription and translation events.
296
297 Mitochondrial proteins regulated through this strategy are enriched for factors involved in the
298 antioxidant response, which is consistent with both the role played by GPS2 in mediating the

299 mitochondrial stress response and the role played by K63 ubiquitination in regulating ribosomal
300 activity in yeast (REF). Recent studies have identified RNA binding proteins, such as Puf3p in
301 yeast, Clu and MDI/Larp in flies, CluH and dAKAP1/LARP4 in mammalian cells, that are involved
302 in the selective regulation of different subsets of nuclear-encoded mitochondrial
303 proteins[14,17,18,52,58–62]. Mitochondrial proteins upregulated in GPS2-KO cells present a significant
304 overlap with the AKAP1/MDI/LARP complex targets, which is responsible for recruiting mRNAs
305 to the outer mitochondrial membrane for import-coupled translation. In contrast, no overlap was
306 observed with transcripts binding to CLUH, an RNA binding protein responsible for the assembly
307 of cytosolic granules promoting the cytosolic synthesis of various mitochondrial proteins. These
308 results suggest that different sets of nuclear-encoded mitochondrial genes might be regulated
309 through independent strategies, with GPS2-controlled K63 ubiquitination being restricted to the
310 local regulation of mitochondria-associated translation. This separation is likely to be critical for
311 ensuring the maintenance of mitochondrial and cellular homeostasis.
312
313 Mechanistically, our results indicate that GPS2 regulates mitochondrial-associated translation by
314 inhibiting the ubiquitination of the RNA binding protein PABPC1 and other translation factors by
315 the mitochondrial E3 ubiquitin ligase Mul1. To our surprise, our data point to the mitochondria-
316 specific Mul1 as the E3 ligase regulating PABPC1 ubiquitination both *in vivo* and *in vitro*, rather
317 than MKRN1, which had been previously associated with the ubiquitination of PABPC1 in
318 HEK293T[54]. Mul1 is a dual function E3 ligase promoting either the ubiquitination or SUMOylation
319 of mitochondrial targets[63,64]. Previous studies have described an important role for Mul1 in
320 regulating a variety of physiological and pathological processes, including mitochondrial
321 dynamics, cell growth, apoptosis, and mitophagy[65–69]. Our study adds to this body of work by
322 showing that Mul1-mediated ubiquitination regulates the activity of translation factors localized to
323 the OMM and restricts the local translation of a subset of nuclear-encoded mitochondrial proteins.
324 One intriguing aspect of Mul1 involvement in regulating mitochondria-associated translation is

325 that it is uniquely suited for playing a key role in the mitochondrial stress response (MSR).
326 Because of its spatial organization, Mul1 can in fact sense mitochondrial stress in the
327 intermembrane mitochondrial space and respond through the ubiquitination of specific substrates
328 on the outer mitochondrial surface[68–70]. Our data support this possibility as we observed increased
329 ubiquitination of PABPC1 upon mitochondrial depolarization, concomitant to GPS2 retrograde
330 translocation to the nucleus.
331
332 The relationship between GPS2 and Mul1 in mitochondria appears quite complex. Mul1 was
333 previously shown to regulate the sumoylation of GPS2, as required for regulating GPS2
334 intracellular localization and translocation in stress conditions[9]. At the same time, results
335 presented here indicate that GPS2 inhibits Ubc13/Mul1-mediated ubiquitination of PABPC1, likely
336 through inhibition of Ubc13 activity. Together, these observations suggest a complex regulatory
337 strategy for modulating mitochondrial adaptation to stress which includes: 1) Mul1-mediated
338 sumoylation of GPS2 is removed by SENP1; 2) desumoylation favors GPS2 translocation to the
339 nucleus where it promotes the transcription of stress response and nuclear-encoded
340 mitochondrial genes; 3) at the same time the absence of GPS2 in mitochondria licenses
341 Mul1/Ubc13 activity on mitochondria-associated translation factors, in turn enhancing the
342 translation of antioxidant proteins to promote adaptation to the mitochondrial stress.
343
344 While we have mainly focused on PABPC1 as a key target of GPS2-regulated ubiquitination in
345 this study, our proteomics data suggest that PABPC1 is not the only target relevant to the
346 regulation of mitochondrial-associated translation. Ribosomes are known to be regulated by non-
347 proteolytic ubiquitination as well, and ribosomal subunit RPS11 and scaffold factor RACK1[71–73].
348 In addition, we identified Eif3m, a translation initiation factor, as a target of GPS2-regulated K63
349 ubiquitination and GPS2. These results suggest that regulation of mitochondrial-associated
350 translation is achieved by the concomitant ubiquitination of multiple factors working together.

351 Further studies will be required to dissect the specific sites of ubiquitination and the contribution
352 of individual PTM events.
353
354 In conclusion, our work indicates that GPS2 plays an important role in mitochondrial regulation
355 by inhibiting ubiquitin signaling. Together with the recent characterization of GPS2-mediated
356 regulation of nuclear-encoded mitochondrial genes transcription, our results add to the
357 significance of the GPS2 role in integrating multiple layers regulating cell growth, metabolism, and
358 stress resistance.
359
360
361 **ACKNOWLEDGMENTS**
362 We thank all past and present members of the Perissi Lab for their continuous support and
363 encouragement. We are grateful to Drs. Christine Vogel and Gustavo Silva for their assistance
364 with protocols for the enrichment of K63 ubiquitinated proteins. Genomic profiling experiments
365 have been run by the Boston University Microarray & Sequencing Resource Core. This work was
366 supported by NIH and Department of Defense grant awards as follows: NIGMS R01GM127625
367 to VP, DoD W81XWH-17-1-0048 to VP, R00GM124458 to SML
368
369
370

371 ***Materials and Methods***

372 **Reagents and antibodies**

373 Anti-GPS2 antibody was generated in rabbit against a peptide representing aa 307-327.
374 Commercial antibodies used were as follows: anti-ubiquitin (P4D1 clone, Cell Signaling
375 Technology), anti-β-tubulin (TUB 2.1 clone, Sigma), anti-HDAC2 (ab16032, Abcam), anti-
376 mtHSP70 (catalog no. MA3-028, Invitrogen), anti-K63 (catalog no. 05-1308, Millipore), anti-α-
377 Tubulin (catalog no. T5168, Sigma), anti-GAPDH (catalog no. MA5-15738, Invitrogen), anti-
378 PABPC1 (ab21060, Abcam), anti-RPS11(NBP2-22289, Novus Biologicals), anti-Rack1 (sc-
379 17754, Santa Cruz Biotechnology), anti-Eif4G (15704-1-AP, Proteintech), anti-Paip1 (sc-365687,
380 Santa Cruz Biotechnology), anti-Paip2 (15583-1-AP, proteintech), anti-Flag-HRP (catalog no.
381 a8592, Sigma), anti-Puromycin (clone 12D10, Millipore), anti-PDHA (ab168379, Abcam), anti-
382 Oxphos (ab110413, Abcam), anti-SOD2 (sc-137254, Santa Cruz Biotechnology). siRNAs against
383 mouse GPS2, UBC13, MKRN1, MUL1, and UBC9 were purchased from Ambion. Nonspecific
384 scrambled siRNA was included as negative controls in each experiment.

385 **Cell culture**

386 Standard molecular cloning, cell culture, and cell transfection experiments were performed as
387 described by J. Sambrook, D. W. Russell, Molecular Cloning: A Laboratory Manual (Cold Spring
388 Harbor Laboratory Press, Cold Spring Harbor, N.Y., ed. 3rd, 2001). For cells transfection,
389 jetPRIME was used following the manufacturer's protocol (Polyplus transfection). Immunostaining
390 was performed following standard protocols on cells fixed in 4% paraformaldehyde in PBS, using
391 Alexa Fluor-conjugated secondary antibodies (Molecular probes).
392 Mouse embryonic fibroblasts (MEFs) cells were maintained in DMEM with 4.5 g/L glucose and L-
393 glutamine and 10% FBS at 37°C and 5% CO_2. Conditional $Gps2^{flox/flox}$ mice were generated by

394 inGenious Targeting Laboratory. Wild-type mice used as control for all analyses presented here
395 were littermates $Gps2^{flox/flox/}CD19Cre^{-}$.
396 MDA-MB-231 breast cancer cells were grown in DMEM with 4.5 g/L glucose and L-glutamine and
397 10% FBS at 37°C and 5% CO_2. MB231 GPS2 KO cells were generated and described
398 previously[47].

399 **Protein extraction, subcellular fractionation, immunoprecipitation and western blotting**

400 For whole cell extraction, cultured cells were pelleted and incubated for 20 minutes on ice in IPH
401 buffer (50 mM Tris HCl [pH 8.0], 250 mM NaCl, 5 mM EDTA, 0.5% NP-40, 0.1mM PMSF, 2mM
402 Na3VO4, 50mM NaF, and 1X protease inhibitors (Sigma Aldrich)). For cytoplasmatic,
403 mitochondrial and nuclear extracts fractionation, cells were pelleted and resuspended in gradient
404 buffer (10 mM HEPES [pH 7.9], 1mM EDTA, 210 mM Mannitol, 70mM Sucrose, 10mM NEM, 50
405 mM NaF, 2 mM Na2VO3, 1mM PMSF and 1x protease inhibitor mixture), then homogenized by
406 syringe followed by low-speed centrifugation for 10 min. The supernatant containing cytosolic
407 proteins was recovered and subjected to high-speed centrifugation to separate the mitochondrial
408 pellet from the cytoplasmic fraction, and the nuclear pellet was lysed for 20 min in high-salt buffer
409 (20 mM Tris-HCL [pH 8.0], 25% glycerol, 420 mM NaCl, 1.5 mM MgCl2, 0.2 mM EDTA, 0.5 mM
410 DTT, 10mM NEM, 50 mM NaF, 2 mM Na3VO4, 1mM PMSF and protease inhibitor mixture). The
411 mitochondrial pellet was incubated for 15 min in lysis buffer (50 mM Tris/HCl [pH 8.0], 300 mM
412 NaCl, 1mM EDTA, 1% Triton X-100, 10mM NEM, 50 mM NaF, 2 mM Na2VO3, 1mM PMSF and
413 protease inhibitor mixture). The concentration of protein extracts was measured using the
414 Bradford assay (Bio-Rad). Extracts were boiled in SDS sample buffer and loaded directly on
415 precast Bio-Rad gels. For immunoprecipitation, protein extracts were incubated with the specific
416 antibody overnight at 4 °C after adjusting the buffer to a final concentration of 150 mM NaCl and
417 0.5% NP-40 and then incubated for 1 h with Protein A-Sepharose™ 4B (Invitrogen), washed

418 extensively, separated by electrophoresis, transferred onto PVDF membranes (Millipore), and
419 subjected to Western blotting following standard protocols.

420 **Recombinant Protein Expression**

421 cDNAs encoding the tandem ubiquitin-binding entity (Vx3K0 and Rx3(A7)) (Sims J., 2012, Nature
422 protocol) were subcloned into pET28a-His-tag expression vector. Human clone of GPS2 and
423 mouse clone of PABPC1 and mutated PABPC1 (with four lysine mutations: K78R, K188R, K284R
424 and K512R) were subcloned into pET-32a-His-tag expression vectors. His-tagged Vx3K0,
425 Rx3(A7), GPS2 and PABPC1 were produced as a His-tag fusion protein in BL21 *Escherichia coli*,
426 resin-purified on nickel-nitrilotriacetic acid beads, and eluted accordingly to manufacturer's
427 protocol (Life Technologies). The His-Vx3K0/Rx3(A7)-conjugated agarose were stored at 4°C in
428 PBS supplemented with 30% glycine.

429 **Immunochemical methods**

430 For pull-down of K63-ubiquitylated proteins, cells were lysed in high-stringency buffer (50 mM
431 Tris, pH 7.5; 500 mM NaCl; 5 mM EDTA; 1% NP40; 1 mM dithiothreitol (DTT); 0.1% SDS)
432 containing 1.25 mg ml−1 N-ethylmaleimide, 0.1% PMSF, and protease inhibitor cocktail (Roche).
433 His-Vx3K0/Rx3(A7) were added to immobilize the K63-ubiquitylated proteins, and bound material
434 was washed extensively in high-stringency buffer four times. Proteins were resolved by SDS-
435 APGE and analyzed by immunoblotting.

436 **In vitro ubiquitination assay**

437 Ubiquitination assays were carried out at 30°C for 2h in 50mM Tris-HCl, pH7.6, containing 50mM
438 NaCl, 5mM MgCl2, 5mM ATP, 1x Ubiquitin Aldheide, 50nM E1, 5μg ubiquitin, 200 nM UbcH13–
439 Uev1a E2 complexes (Boston Biochem), 0.1ug recombinant human MUL1 Protein (H00079594-

440 P01, Novus Biologicals). Bacterial expressed His-PABPC1/mutated PABPC1 was used as
441 substrate.

442 **Mitochondrial RNA Isolation and RNA-seq**

443 Mitochondrial RNA was isolated from isolated mitochondrial pellet following the manufacturer
444 protocol for the RNeasy Kit (QIAGEN). Isolated mitochondrial RNA was subjected to quality
445 control on Agilent Bioanalyzer and RNA library preparation following Illumina's RNA-seq Sample
446 Preparation Protocol. Resulting cDNA libraries were sequenced on the Illumina's HiSeq 2000.

447 **Mitochondrial Content**

448 Total DNA was extracted from cells using QuickExtract DNA Extraction Solution 1.0 (Epicenter)
449 following manufacturer's instructions. DNA amplification of the mitochondrial-encoded NADH
450 dehydrogenase 1 (mt-ND1) relative to nuclear TFAM was used to determine mitochondrial DNA
451 copy number.

452 **Translation activity**

453 Puromycin incorporation into newly synthesized proteins was performed to measure translation
454 activity. MEFs WT and GPS2-KO cells were treated in the presence or absence of
455 homoharringtonine (HHT) (5 μM, Tocris Bioscience) for 10 min to prevent new translation
456 initiation, prior to an additional 5 min incubation with puromycin (100 μM, Sigma) and emetine
457 (200 μM, Sigma) at 37°C. Cells were collected by centrifugation, and lysate was prepared as
458 described above. Thirty micrograms of protein were loaded onto a 10% SDS-PAGE gel for
459 immunoblotting analysis.

460 **Sample preparation for MS analysis**

461 For mitochondrial proteome profiling, mitochondrial proteins from MEFs WT and GPS2-KO cells
462 were isolated as described before[9]. An equal amount of solubilized mitochondrial proteins from
463 different samples were separated by SDS-PAGE and then digested in-gel by trypsin overnight
464 using standard methods[74].
465 For SILAC-K63 experiments, MEFs WT and GPS2-KO cells or MDA-MB231 WT and GPS2-KO
466 cells were grown in medium containing native (unlabeled) L-arginine and L-lysine (Arg0/Lys0) as
467 the light condition, or stable isotope-labelled variants of L-arginine and L-lysine (Arg10/Lys8) as
468 the heavy condition[75]. Proteins from whole cellular lysates were extracted from SILAC-labelled
469 MEFs WT and GPS2-KO cells or MDA-MB-231WT and GPS2-KO cells as descripted before. An
470 equal amount of proteins from the two SILAC states was mixed and precipitated by His-Vx3K0-
471 conjugated agarose and incubating at 4°C for 1h. Precipitated proteins were eluted with SDS
472 sample buffer, incubated with 10 mM DTT for 10min at 100 °C. Proteins were separated by SDS-
473 PAGE and then digested in-gel by trypsin overnight using standard methods. The resulting
474 peptides were desalted using reverse phase (C18) Tips (Thermo Scientific) per the
475 manufacturer's instructions.
476 For TMT based-K63 experiments, MEFs WT and GPS2-KO cells were grown in normal medium
477 to 80% confluency. After lysis with IPH buffer, protein quantities from whole cellular lysates were
478 determined using the Bradford assay. An equal amount of proteins from MEFs WT or GPS2-KO
479 cells was precipitated by His-Vx3K0-conjugated agarose and incubating at 4°C for 1h.
480 Precipitated proteins were eluted with SDS sample buffer, incubated with 10 mM DTT for 10min
481 at 100 °C. Proteins were separated by SDS-PAGE and then digested in-gel by trypsin overnight
482 using standard methods. The resulting peptides were desalted using C18 Tips (Thermo Scientific)
483 per the manufacturer's instructions and vacuum-dried. The dried peptides were redissolved in 0.5
484 M TEAB, and processed independently according to the manufacturer's protocol for a 10-plex

485 Tandem Mass Tag (TMT) reagent labeling kit (Thermo Fisher Scientific). The different TMT-
486 labeled peptide mixtures were pooled equally, desalted and dried by vacuum centrifugation.

487 **Mass spectrometric analysis**

488 Peptides were analyzed on a Q-Exactive HF mass spectrometer (QE-HF, Thermo Fisher
489 Scientific) equipped with a nanoflow EasyLC1200 HPLC system (Thermo Fisher Scientific).
490 Peptides were loaded onto a C18 trap column (3 µm, 75 µm × 2 cm, Thermo Fisher Scientific)
491 connected in-line to a C18 analytical column (2 µm, 75 µm × 50 cm, Thermo EasySpray) using
492 the Thermo EasyLC 1200 system with the column oven set to 55 °C. The nanoflow gradient
493 consisted of buffer A (composed of 2% (v/v) ACN with 0.1% formic acid) and buffer B (consisting
494 of 80% (v/v) ACN with 0.1% formic acid). For protein analysis, nLC was performed for 180 min at
495 a flow rate of 250 nL/min, with a gradient of 2-8% B for 5 min, followed by a 8-20% B for 96 min,
496 a 20-35% gradient for 56min, and a 35-98% B gradient for 3 min, 98% buffer B for 3 min, 100-0%
497 gradient of B for 3 min, and finishing with 5% B for 14 min. Peptides were directly ionized using a
498 nanospray ion source and analyzed on the Q-Exactive HF mass spectrometer (Thermo Fisher
499 Scientific).
500 QE-HF was run using data dependent MS2 scan mode, with the top 10 most intense precursor
501 ions acquired per profile mode full-scan precursor mass spectrum subject to HCD fragmentation.
502 Full MS spectra were collected at a resolution of 120,000 with an AGC of 3e6 or maximum
503 injection time of 60 ms and a scan range of 350 to 1650 m/z, while the MS2 scans were performed
504 at 45,000 resolution, with an ion-packet setting of 2e4 for AGC, maximum injection time of 90 ms,
505 and using 33% NCE. Source ionization parameters were optimized with the spray voltage at 2.1
506 kV, transfer temperature at 275 °C. Dynamic exclusion was set to 40 seconds.

507 **Data analysis**

508 All acquired MS/MS spectra were searched against the Uniprot mouse complete proteome
509 FASTA database released on 2013_07_01, using the MaxQuant software (Version 1.6.7.0) that
510 integrates the Andromeda search engine. Enzyme specificity was set to trypsin and up to two
511 missed cleavages were allowed. Cysteine carbamidomethylation was specified as a fixed
512 modification. Methionine oxidation, N-terminal acetylation, and lysine ubiquitination were included
513 as variable modifications. Peptide precursor ions were searched with a maximum mass deviation
514 of 6 ppm and fragment ions with a maximum mass deviation of 20 ppm. Peptide and protein
515 identifications were filtered at 1% FDR using the target-decoy database search strategy. Proteins
516 that could not be differentiated based on MS/MS spectra alone were grouped to protein groups
517 (default MaxQuant settings). For mitochondrial protein annotation, we utilized the latest Mitocarta
518 dataset(https://www.broadinstitute.org/files/shared/metabolism/mitocarta/human.mitocarta3.0.ht
519 ml).

520 **Statistical analysis**

521 The statistical data are from three independent experiments. Results are shown as mean ± SEM
522 unless mentioned otherwise. Statistical analysis was performed by the Student's t-test for TMT-
523 based quantification and RNA-seq data.
524
525
526

527 **REFERENCES**

528 1. Palikaras, K. & Tavernarakis, N. Mitochondrial homeostasis: The interplay between
529 mitophagy and mitochondrial biogenesis. *Experimental Gerontology* **56**, 182–188 (2014).
530 2. RS, I., E, M. & LS, C. The Multiple Levels of Mitonuclear Coregulation. *Annual review of*
531 *genetics* **52**, 511–533 (2018).
532 3. Quirós, P. M., Mottis, A. & Auwerx, J. Mitonuclear communication in homeostasis and
533 stress. *Nature Reviews Molecular Cell Biology* **17**, 213–226 (2016).
534 4. English, J., Son, J. M., Cardamone, M. D., Lee, C. & Perissi, V. Decoding the Rosetta
535 Stone of Mitonuclear Communication. *Pharmacological Research* 105161 (2020)
536 doi:10.1016/j.phrs.2020.105161.
537 5. Woodson, J. D. & Chory, J. Coordination of gene expression between organellar and
538 nuclear genomes. *Nature Reviews Genetics* vol. 9 383–395 (2008).
539 6. AM, N., MW, P., CJ, F., BM, B. & CM, H. Mitochondrial import efficiency of ATFS-1
540 regulates mitochondrial UPR activation. *Science (New York, N.Y.)* **337**, 587–590 (2012).
541 7. CJ, F. *et al.* The Transcription Factor ATF5 Mediates a Mammalian Mitochondrial UPR.
542 *Current biology : CB* **26**, 2037–2043 (2016).
543 8. S, A. *et al.* MNRR1 (formerly CHCHD2) is a bi-organellar regulator of mitochondrial
544 metabolism. *Mitochondrion* **20**, 43–51 (2015).
545 9. Cardamone, M. D. *et al.* Mitochondrial Retrograde Signaling in Mammals Is Mediated by
546 the Transcriptional Cofactor GPS2 via Direct Mitochondria-to-Nucleus Translocation.
547 *Molecular Cell* **69**, 757-772.e7 (2018).
548 10. MT, C., IC, S., G, S. & LS, C. Synchronized mitochondrial and cytosolic translation
549 programs. *Nature* **533**, 499–503 (2016).
550 11. Margeot, A. & al., et. Why are many mRNAs translated to the vicinity of mitochondria: a
551 role in protein complex assembly? *Gene* **354**, 64–71 (2005).
552 12. Chacinska, A. & al., et. Importing mitochondrial proteins: machineries and mechanisms.
553 *Cell* **138**, 628–644 (2009).
554 13. Bykov, Y. S., Rapaport, D., Herrmann, J. M. & Schuldiner, M. Cytosolic Events in the
555 Biogenesis of Mitochondrial Proteins. *Trends in Biochemical Sciences* **45**, 650–667
556 (2020).
557 14. J, G. *et al.* CLUH regulates mitochondrial biogenesis by binding mRNAs of nuclear-
558 encoded mitochondrial proteins. *The Journal of cell biology* **207**, 213–223 (2014).
559 15. Schatton, D. *et al.* CLUH regulates mitochondrial metabolism by controlling translation
560 and decay of target mRNAs. *The Journal of cell biology* **216**, 675–693 (2017).

561 16. Pla-Martín, D. *et al.* CLUH granules coordinate translation of mitochondrial proteins with
562 mTORC1 signaling and mitophagy. *The EMBO Journal* **39**, (2020).
563 17. Schatton, D. & Rugarli, E. I. A concert of RNA-binding proteins coordinates mitochondrial
564 function. *Critical Reviews in Biochemistry and Molecular Biology* **53**, 652–666 (2018).
565 18. Y, Z., Y, C., M, G. & H, X. The mitochondrial outer membrane protein MDI promotes local
566 protein synthesis and mtDNA replication. *The EMBO journal* **35**, 1045–1057 (2016).
567 19. A, S. & RT, C. Clueless is a conserved ribonucleoprotein that binds the ribosome at the
568 mitochondrial outer membrane. *Biology open* **5**, 195–203 (2016).
569 20. LJ, G.-R., AC, G. & LA, P. Puf3p, a Pumilio family RNA binding protein, localizes to
570 mitochondria and regulates mitochondrial biogenesis and motility in budding yeast. *The*
571 *Journal of cell biology* **176**, 197–207 (2007).
572 21. García-Rodríguez, L. J. & al., et. Puf3p, a Pumilio family RNA binding protein, localizes to
573 mitochondria and regulates mitochondrial biogenesis and motility in budding yeast. *J. Cell*
574 *Biol.* **176**, 197–207 (2007).
575 22. Garcia, M. & al., et. Mitochondria-associated yeast mRNAs and the biogenesis of
576 molecular complexes. *Mol. Biol. Cell* **18**, 362–368 (2006).
577 23. Williams, C. C. & al., et. Targeting and plasticity of mitochondrial proteins revealed by
578 proximity-specific ribosome profiling. *Science* **346**, 748–751 (2014).
579 24. CM, P. Mechanisms underlying ubiquitination. *Annual review of biochemistry* **70**, 503–
580 533 (2001).
581 25. CE, B. & C, W. New insights into ubiquitin E3 ligase mechanism. *Nature structural &*
582 *molecular biology* **21**, 301–307 (2014).
583 26. Kravtsova-Ivantsiv, Y. & Ciechanover, A. Non-canonical ubiquitin-based signals for
584 proteasomal degradation. *Journal of Cell Science* **125**, 539–548 (2012).
585 27. M, A., I, D. & A, B. Ubiquitin chain diversity at a glance. *Journal of cell science* **129**, 875–
586 880 (2016).
587 28. F, I., N, C. & I, D. What determines the specificity and outcomes of ubiquitin signaling?
588 *Cell* **143**, 677–681 (2010).
589 29. Chen, Z. J. & Sun, L. J. Nonproteolytic Functions of Ubiquitin in Cell Signaling. *Molecular*
590 *Cell* **33**, 275–286 (2009).
591 30. Mukhopadhyay, D. & Riezman, H. Proteasome-independent functions of ubiquitin in
592 endocytosis and signaling. *Science* **315**, 201–205 (2007).
593 31. J, S. *et al.* Cell cycle-regulated modification of the ribosome by a variant multiubiquitin
594 chain. *Cell* **102**, 67–76 (2000).

595 32. F, H. *et al.* Lysine 63-linked polyubiquitination is required for EGF receptor degradation.
596 *Proceedings of the National Academy of Sciences of the United States of America* **110**,
597 15722–15727 (2013).
598 33. E, L., C, J. & B, A. K63-linked ubiquitin chains as a specific signal for protein sorting into
599 the multivesicular body pathway. *The Journal of cell biology* **185**, 493–502 (2009).
600 34. GS, S. *et al.* The RIDDLE syndrome protein mediates a ubiquitin-dependent signaling
601 cascade at sites of DNA damage. *Cell* **136**, 420–434 (2009).
602 35. C, D. *et al.* RNF168 binds and amplifies ubiquitin conjugates on damaged chromosomes
603 to allow accumulation of repair proteins. *Cell* **136**, 435–446 (2009).
604 36. C, H., B, P., GL, M., G, P. & S, J. RAD6-dependent DNA repair is linked to modification of
605 PCNA by ubiquitin and SUMO. *Nature* **419**, 135–141 (2002).
606 37. MU, G. *et al.* TRIM25 RING-finger E3 ubiquitin ligase is essential for RIG-I-mediated
607 antiviral activity. *Nature* **446**, 916–920 (2007).
608 38. IC, P. & W, S. Functional implications of K63-linked ubiquitination in the iron deficiency
609 response of Arabidopsis roots. *Frontiers in plant science* **4**, (2014).
610 39. Dougherty, S. E., Maduka, A. O., Inada, T. & Silva, G. M. Expanding role of ubiquitin in
611 translational control. *International Journal of Molecular Sciences* **21**, (2020).
612 40. Zhou, Y. *et al.* Structural impact of K63 ubiquitin on yeast translocating ribosomes under
613 oxidative stress. *Proceedings of the National Academy of Sciences of the United States*
614 *of America* **117**, 22157–22166 (2020).
615 41. S, B., AW, G., C, V. & GM, S. Site-Specific K63 Ubiquitinomics Provides Insights into
616 Translation Regulation under Stress. *Journal of proteome research* **18**, 309–318 (2019).
617 42. GM, S., D, F. & C, V. K63 polyubiquitination is a new modulator of the oxidative stress
618 response. *Nature structural & molecular biology* **22**, 116–123 (2015).
619 43. L, W. *et al.* Arabidopsis UBC13 differentially regulates two programmed cell death
620 pathways in responses to pathogen and low-temperature stress. *The New phytologist*
621 **221**, 919–934 (2019).
622 44. Lentucci, C. *et al.* Inhibition of Ubc13-mediated Ubiquitination by GPS2 Regulates
623 Multiple Stages of B Cell Development. *Journal of Biological Chemistry* **292**, (2017).
624 45. Cardamone, M. *et al.* A Protective Strategy against Hyperinflammatory Responses
625 Requiring the Nontranscriptional Actions of GPS2. *Molecular Cell* **46**, (2012).
626 46. Cederquist, C. T. *et al.* Systemic insulin sensitivity is regulated by GPS2 inhibition of AKT
627 ubiquitination and activation in adipose tissue. *Molecular Metabolism* **6**, 125–137 (2017).

628 47. Chan, S. *et al.* Loss of G-Protein Pathway Suppressor 2 Promotes Tumor Growth
629 Through Activation of AKT Signaling. *Frontiers in Cell and Developmental Biology* **8**,
630 (2021).
631 48. Cardamone, M. *et al.* GPS2/KDM4A pioneering activity regulates promoter-specific
632 recruitment of PPARγ. *Cell Reports* **8**, (2014).
633 49. Sims, J. J. *et al.* Polyubiquitin-sensor proteins reveal localization and linkage-type
634 dependence of cellular ubiquitin signaling. *Nature methods* **9**, 303 (2012).
635 50. Wetzler, M. & Segal, D. Omacetaxine as an Anticancer Therapeutic: What is Old is New
636 Again. *Current Pharmaceutical Design* **17**, 59–64 (2011).
637 51. Z, W. *et al.* Ubiquitination of ABCE1 by NOT4 in Response to Mitochondrial Damage
638 Links Co-translational Quality Control to PINK1-Directed Mitophagy. *Cell metabolism* **28**,
639 130-144.e7 (2018).
640 52. L, G. *et al.* A-kinase-anchoring protein 1 (dAKAP1)-based signaling complexes
641 coordinate local protein synthesis at the mitochondrial surface. *The Journal of biological*
642 *chemistry* **295**, 10749–10765 (2020).
643 53. D, P.-M. *et al.* CLUH granules coordinate translation of mitochondrial proteins with
644 mTORC1 signaling and mitophagy. *The EMBO journal* **39**, (2020).
645 54. Hildebrandt, A. *et al.* The RNA-binding ubiquitin ligase MKRN1 functions in ribosome-
646 associated quality control of poly(A) translation. *Genome Biology 2019 20:1* **20**, 1–20
647 (2019).
648 55. Sonenberg, N. & Hinnebusch, A. G. Regulation of Translation Initiation in Eukaryotes:
649 Mechanisms and Biological Targets. *Cell* **136**, 731 (2009).
650 56. A, K., YV, S., R, S., MN, M. & N, S. Mammalian poly(A)-binding protein is a eukaryotic
651 translation initiation factor, which acts via multiple mechanisms. *Genes & development*
652 **19**, 104–113 (2005).
653 57. Yoshida, M. *et al.* Poly(A) binding protein (PABP) homeostasis is mediated by the stability
654 of its inhibitor, Paip2. *The EMBO Journal* **25**, 1934 (2006).
655 58. Schäffler, K. *et al.* A stimulatory role for the La-related protein 4B in translation. *Rna* **16**,
656 1488–1499 (2010).
657 59. Lesnik, C., Golani-Armon, A. & Arava, Y. Localized translation near the mitochondrial
658 outer membrane: An update. *RNA Biology* **12**, 801–809 (2015).
659 60. Stavraka, C. & Blagden, S. The La-related proteins, a family with connections to cancer.
660 *Biomolecules* **5**, 2701–2722 (2015).

661 61. Eliyahu, E. *et al.* Tom20 Mediates Localization of mRNAs to Mitochondria in a
662 Translation-Dependent Manner. *Molecular and Cellular Biology* **30**, 284–294 (2010).
663 62. Schatton, D. *et al.* CLUH regulates mitochondrial metabolism by controlling translation
664 and decay of target mRNAs. *The Journal of Cell Biology* **216**, 675–693 (2017).
665 63. E, B., R, Z. & HM, M. MAPL is a new mitochondrial SUMO E3 ligase that regulates
666 mitochondrial fission. *EMBO reports* **10**, 748–754 (2009).
667 64. J, P., KD, R., J, Y. & XJ, L. Mitochondrial E3 ubiquitin ligase 1: A key enzyme in
668 regulation of mitochondrial dynamics and functions. *Mitochondrion* **28**, 49–53 (2016).
669 65. M, E.-H. & M, J. Mitofusins: Disease Gatekeepers and Hubs in Mitochondrial Quality
670 Control by E3 Ligases. *Frontiers in physiology* **10**, (2019).
671 66. R, P., XT, C., MY, L., N, H. & ZH, S. Mul1 restrains Parkin-mediated mitophagy in mature
672 neurons by maintaining ER-mitochondrial contacts. *Nature communications* **10**, (2019).
673 67. R, P., XT, C., MY, L., N, H. & ZH, S. Defending stressed mitochondria: uncovering the
674 role of MUL1 in suppressing neuronal mitophagy. *Autophagy* **16**, 176–178 (2020).
675 68. Neutzner, A., Benard, G., Youle, R. J. & Karbowski, M. Role of the ubiquitin conjugation
676 system in the maintenance of mitochondrial homeostasis. *Annals of the New York*
677 *Academy of Sciences* **1147**, 242–253 (2008).
678 69. Peng, J., Ren, K. di, Yang, J. & Luo, X. J. Mitochondrial E3 ubiquitin ligase 1: A key
679 enzyme in regulation of mitochondrial dynamics and functions. *Mitochondrion* **28**, 49–53
680 (2016).
681 70. W, L. *et al.* Genome-wide and functional annotation of human E3 ubiquitin ligases
682 identifies MULAN, a mitochondrial E3 that regulates the organelle's dynamics and
683 signaling. *PloS one* **3**, (2008).
684 71. Y, Z. *et al.* Structural impact of K63 ubiquitin on yeast translocating ribosomes under
685 oxidative stress. *Proceedings of the National Academy of Sciences of the United States*
686 *of America* **117**, 22157–22166 (2020).
687 72. Back, S., Gorman, A. W., Vogel, C. & Silva, G. M. Site-Specific K63 Ubiquitinomics
688 Provides Insights into Translation Regulation under Stress. *Journal of Proteome*
689 *Research* **18**, 309–318 (2019).
690 73. F, B. *et al.* Comprehensive analysis of the ubiquitinome during oncogene-induced
691 senescence in human fibroblasts. *Cell cycle (Georgetown, Tex.)* **14**, 1540–1547 (2015).
692 74. Jensen, O. N., Wilm, M., Shevchenko, A. & Mann, M. Sample Preparation Methods for
693 Mass Spectrometric Peptide Mapping Directly from 2-DE Gels. *Methods in molecular*
694 *biology (Clifton, N.J.)* **112**, 513–530 (1999).

75. Ong, S. E. *et al.* Stable isotope labeling by amino acids in cell culture, SILAC, as a simple and accurate approach to expression proteomics. *Molecular & cellular proteomics : MCP* **1**, 376–386 (2002).

700 **FIGURE LEGENDS**

701

702 **Figure 1 - Mitochondrial proteome of GPS2 WT and KO MEFs**

703

704 A, Heatmap showing 137 significantly changed mitochondrial proteins induced by GPS2-
705 deficiency from GPS2 WT and KO MEFs. Enriched biological process GO terms of significantly
706 downregulated (blue, upper panels) or upregulated (red, down panels) in response to GPS2
707 deficiency.

708 B, Western blot analysis of SOD2, PDRX2, and FASN normalized to GAPDH in mitochondrial
709 extracts from WT versus GPS2 KO MEFs.

710 C&D, Distribution of 137 significantly changed mitochondrial proteins based on LC-MS/MS
711 analysis and RNA-seq (C) or previously generated GRO-seq in 3T3-L1 cells[9]. Red, upregulated
712 proteins identified through RNA-seq and proteomics; Blue, upregulated proteins identified through
713 proteomics, but downregulated in RNA-seq; Black, downregulated proteins identified through
714 proteomics.

715

716 **Figure 2 - K63 ubiquitome profiling of GPS2 WT and KO MEFs by LC-MS/MS**

717 A, Increased K63 ubiquitination in mitochondria extract in GPS2 KO compared to WT by western
718 blot.

719 B, SILAC-based K63 proteomic profiling of GPS2 WT and KO MEFs.

720 C, Gene ontology analysis of 46 putative K63 ubiquitinated proteins whose ubiquitination is
721 mediated by GPS2.

722 D, Detection of K63 ubiquitination of RPS11 and RACK1 purified by specific K63-ubiquitin binding
723 domain Vx3K0 by IP/WB using both whole-cell extracts and fractionated mitochondrial extracts in
724 GPS2 WT and KO MEFs.

725 E, Puromycin labeling of *de novo* protein synthesis on different fractionated extracts pretreated
726 w/o homoharringtonine (HHT). ME, mitochondrial extract; CE, cytosol extract; NE, nuclear extract;
727 WCL, whole cell extract. Cells were treated with HHT for 10 min prior to treatment with 0.9mM
728 puromycin for additional 5 min. Anti-GAPDH/B-Tub/HDAC2 blot was used as loading control for
729 different fractions.
730
731 **Figure 3 - PABPC1 ubiquitination is mediated by Mul1 on mitochondria.**
732 A, Detection of K63 ubiquitination of PABPC1 purified by specific K63-ubiquitin binding domain
733 Vx3K0 by IP/WB using both whole cell extracts and fractionated mitochondrial extracts in GPS2
734 WT and KO MEFs.
735 B, Detection of K63 ubiquitination by IP/WB of PABPC1 in mitochondria extracts in GPS2 WT,
736 KO and KO treatment with UBC13 inhibitor MEFs.
737 C, FCCP-induced ubiquitination of PABPC1 is mediated by mitochondria specific E3 ligase MUL1.
738 D, PABPC1 is polyubiquitinated by the E3 ubiquitin ligase MUL1 by *in vitro* ubiquitination assay.
739 E, Polyubiquitination on PABPC1 mediated by E3 ubiquitina ligase MUL1 is significantly inhibited
740 by GPS2 in *in vitro* ubiquitination assay.
741 F, WB analysis of binding of PABPC1 with EIF4G, PAIP1 and PAIP2 on mitochondrial extracts
742 from GPS2 WT and KO MEFs.
743 G, WB analysis of binding of PABPC1 with PAIP1 and PAIP2 on mitochondrial extracts from
744 GPS2 WT, KO and KO knockdown MUL1 (siMul1) MEFs.
745 H, Puromycin labeling of *de novo* protein synthesis on mitochondrial extracts from GPS2 WT, KO
746 and KO knockdown MUL1 (siMul1) MEFs. Anti-GAPDH blot was used as loading control.
747
748 **Figure 4 - K63 ubiquitination-mediated regulation of mitochondrial-associated translation**
749 **in stress response**

750 A, WB of fractionated extracts showing mitochondria-to-nucleus translocation of GPS2 in MEFs
751 cells upon FCCP treatment.
752 B, Detection of K63 ubiquitination by IP/WB of PABPC1 in mitochondria extracts in MEFs cells
753 upon FCCP treatment.
754 C, Detection of K63 ubiquitination of PABPC1 purified by specific K63-ubiquitin binding domain
755 Vx3K0 by IP/WB in mitochondria extracts in MEFs cells upon FCCP treatment.
756 D, WB analysis of binding of PABPC1 with PAIP1 and PAIP2 in mitochondria extracts in MEFs
757 cells upon FCCP treatment.
758 E, Heatmap showing significantly changed mitochondrial proteins in GPS2 WT, KO MEFS and
759 WT cells treated with FCCP for 3h and 12h .
760 F, Western blot analysis of SOD2 normalized to GAPDH in mitochondrial extracts in MEFs cells
761 upon FCCP treatment.
762
763
764 **Supplemental Figure 1, Related to Figure 1**
765 A, Western blot analysis of GPS2 expression in GPS2 WT and KO MEFs cells. Anti-a-Tub blot
766 was used as loading control.
767 B, Mitochondrial DNA content in WT and GPS2 KO MEFs cells. **indicate p-value<0.01.
768 C, Gene ontology analysis of 891 differentially expressed proteins induced by GPS2-deficiency
769 from GPS2 WT and KO MEFs.
770
771 **Supplemental Figure 2, Related to Figure 2**
772 A, Comparison of the binding affinity of Vx3K0 and Rx3 to different type and length ubiquitin
773 chains.
774 B, WB analysis of K63 ubiquitinated proteins captured by Vx3K0 from whole cell extracts in GPS2
775 WT and KO MEFs.

776 C, Scatter plotting analysis of SILAC data obtained from two independent SILAC-K63 ubiquitome
777 experiments. The KO/WT SILAC ratio of two labeled samples were converted to log2 scale for
778 analysis. The proteins identified by SILAC-K63 ubiquitome and their SILAC ratios are listed in
779 supplemental Table 3.
780 D, TMT labeling-based K63 proteomic profiling of GPS2 WT and KO MEFs. Each sample
781 (WT/KO) has 3 replicates for LC-MS/MS analysis.
782 E, Gene ontology analysis of 22 putative K63 ubiquitinated proteins whose ubiquitination are
783 mediated by GPS2 identified in MB231.
784
785 **Supplemental Figure 3, Related to Figure 2**
786 A, Venn diagram comparing identified putative K63 ubiquitinated proteins whose ubiquitination
787 are mediated by GPS2 from MEFs SILAC, MEFs TmT and MDA-MB231 SILAC datasets.
788 B, Detection of K63 ubiquitination of eif3M purified by specific K63-ubiquitin binding domain
789 Vx3K0 by IP/WB using fractionated mitochondrial extracts in GPS2 WT, KO and KO knockdown
790 Mulan (siMul1) MEFs.
791
792
793
794
795

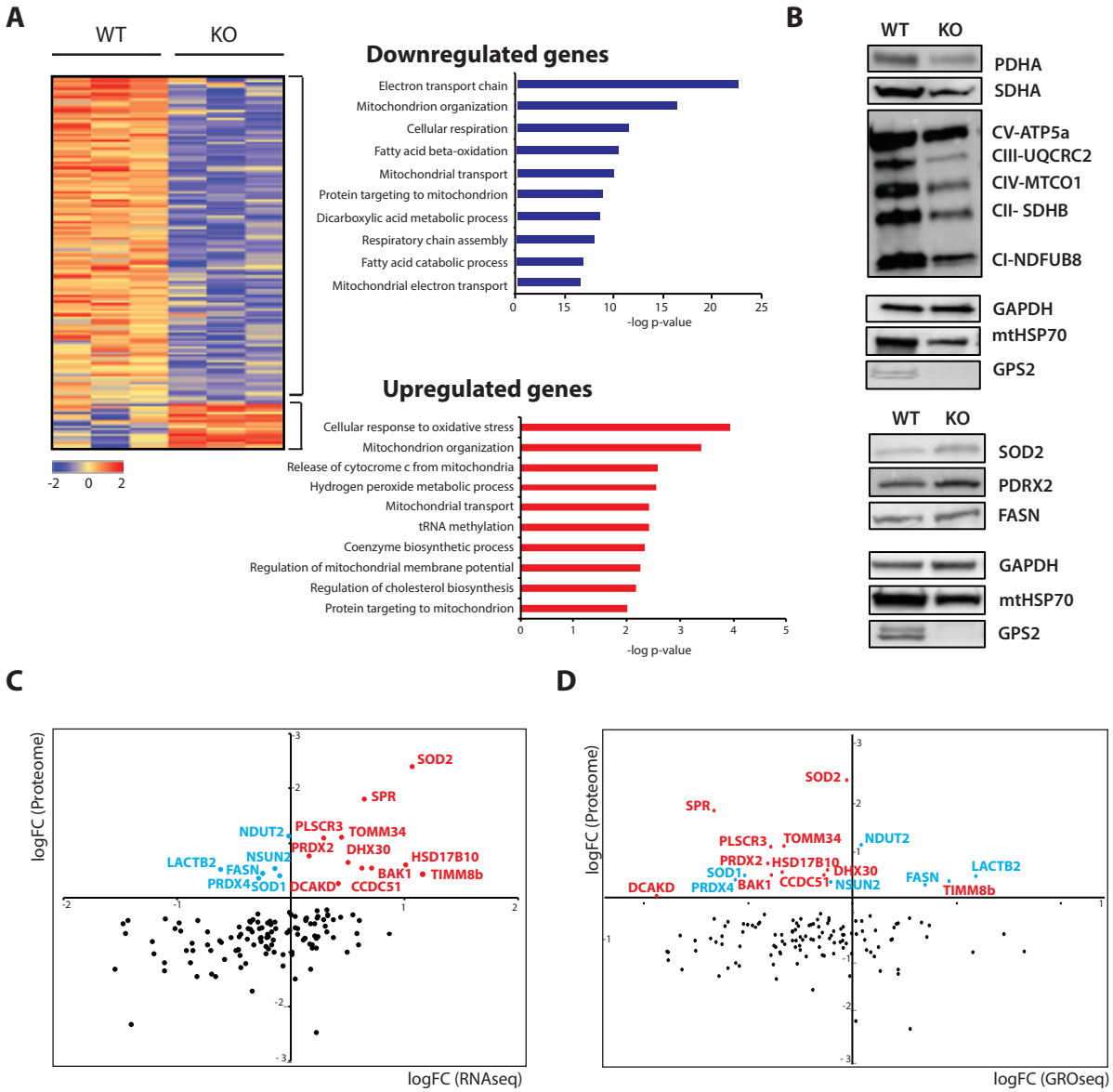

Figure 1

Gao et al., 2021

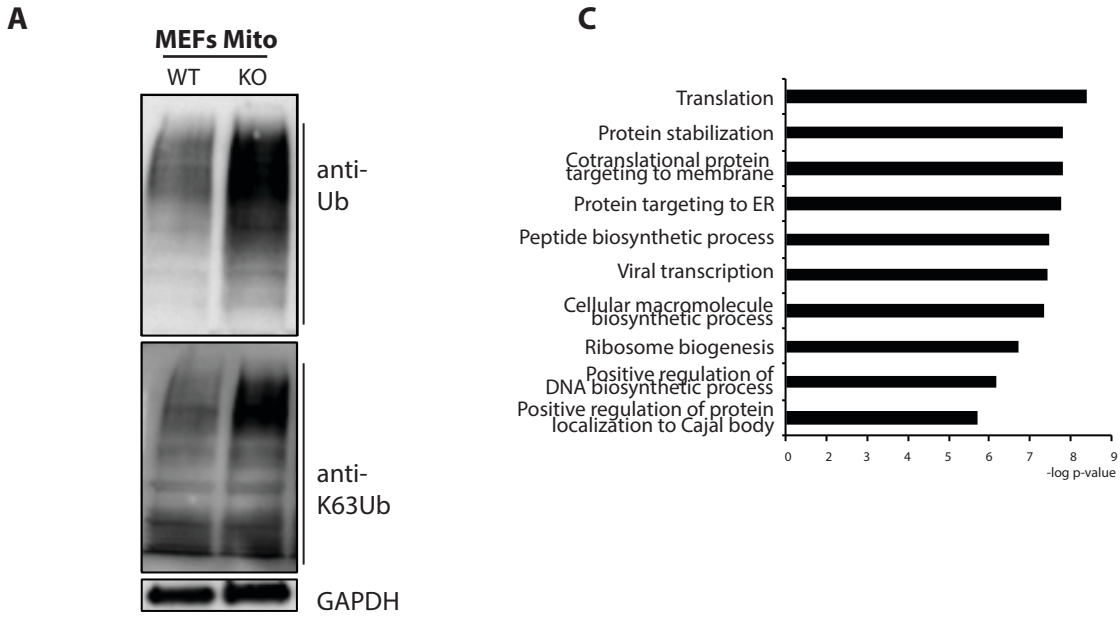

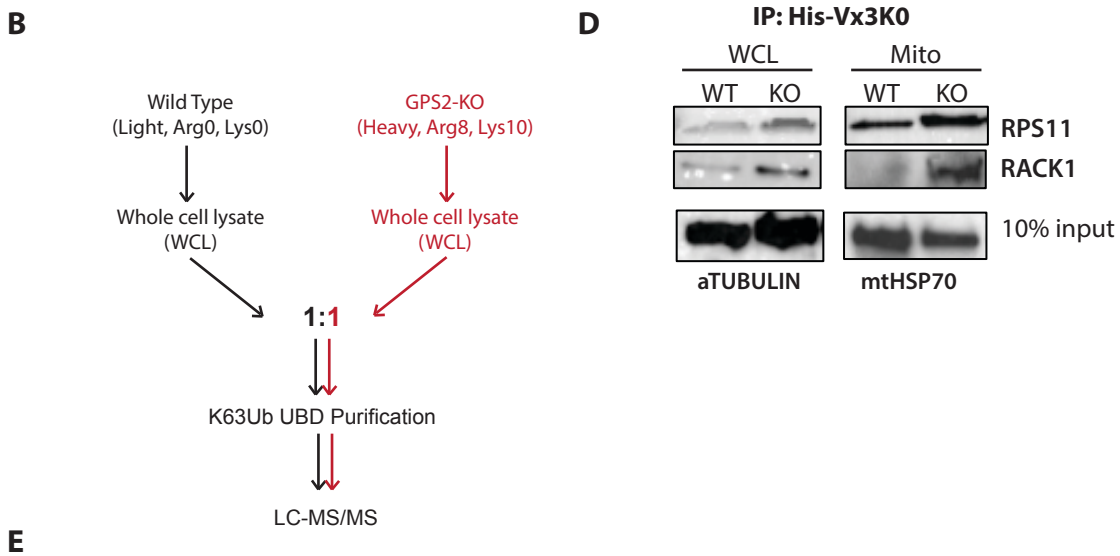

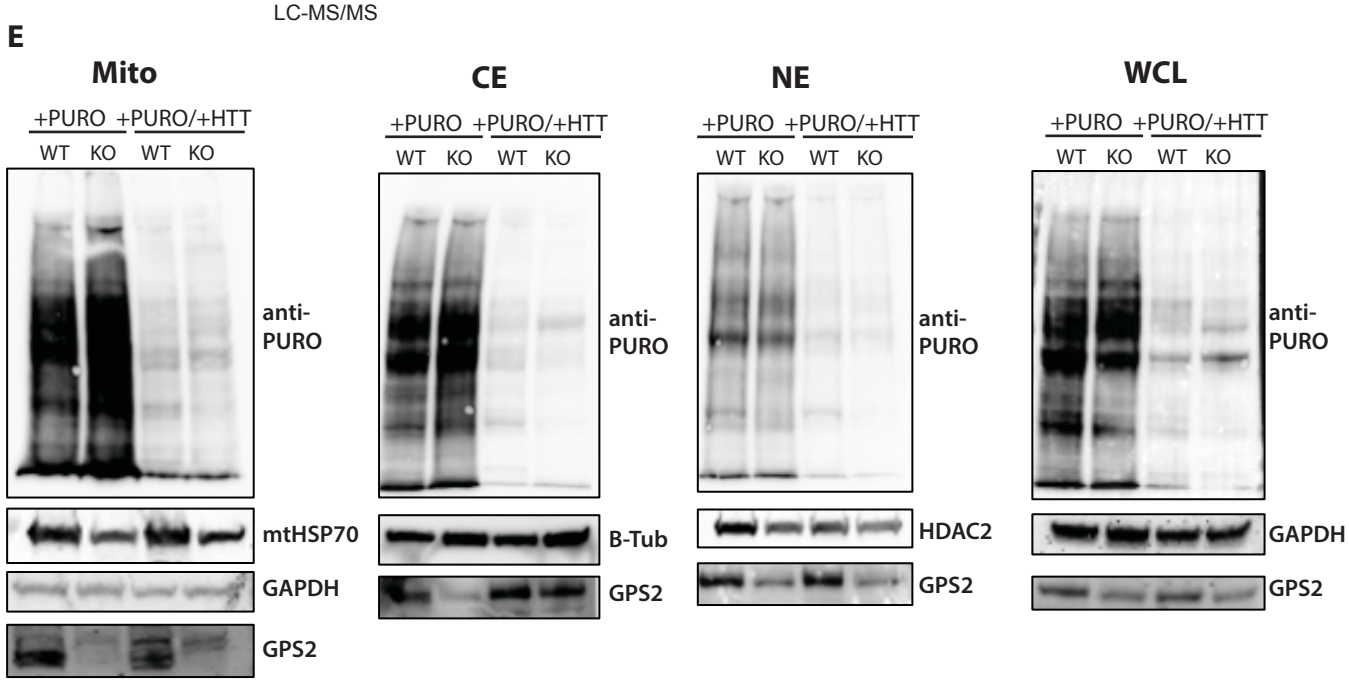

Figure 2

Gao et al., 2021

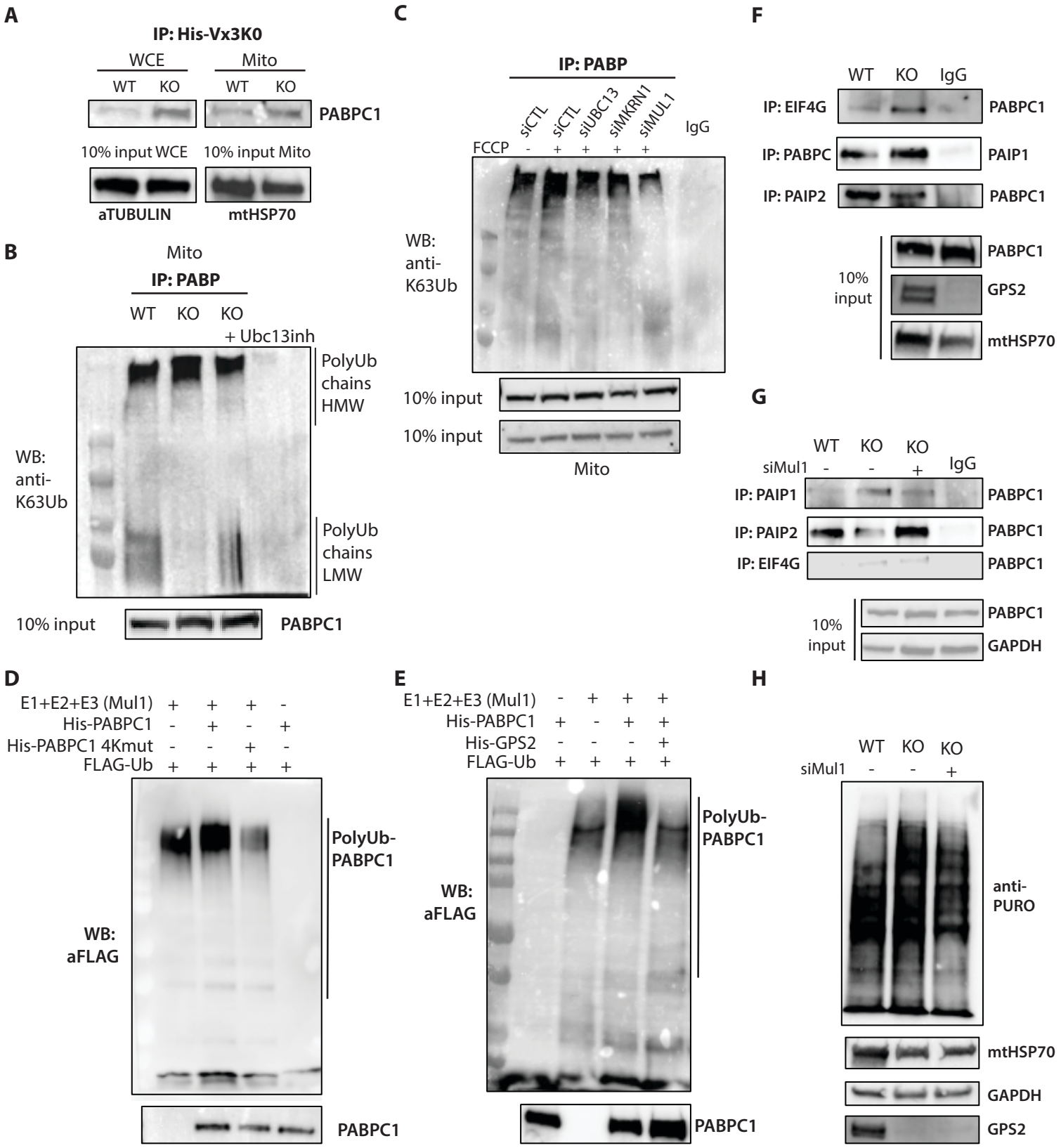

Figure 3
Gao et al., 2021

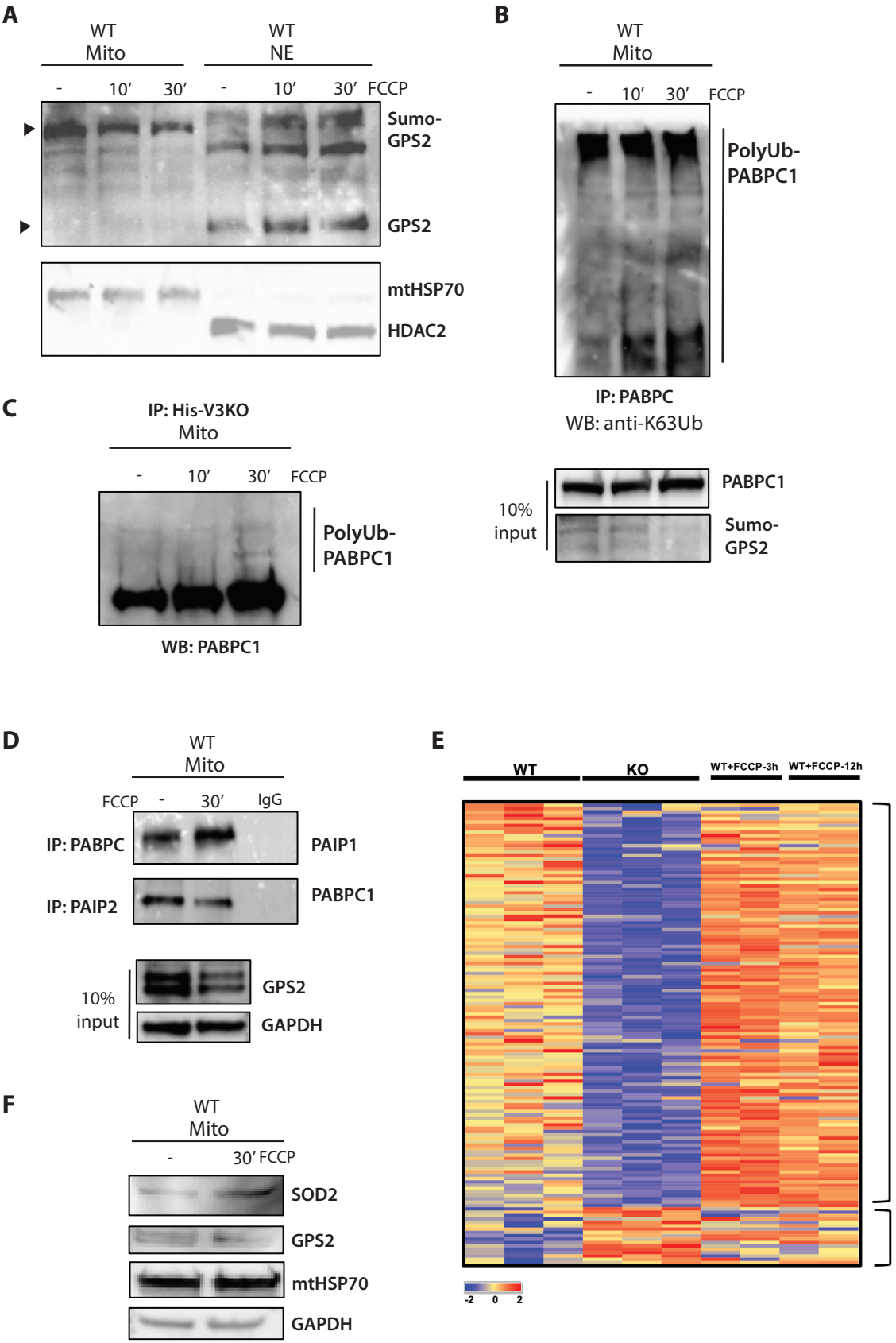

Figure 4
Gao et al., 2021